ISSN 214-453-2

ELECTRICAL CONDUCTION AND DIELECTRIC LOSS CHARACTERISTICS IN NATURAL ESTER DIELECTRIC FLUID

A. A. ABDELMALIK
Department of Physics, Ahmadu Bello University Zaria, Nigeria
[aaabdelmalik@gmail.com]

ABSTRACT
Alkyl ester derivatives of palm kernel oil have been prepared for use as bio-dielectrics in oil filled High Voltage (HV) electric equipment. Electrical conduction and loss characteristics of the ester derivatives were studied to understand the behaviour of the material under applied electric field. Frequency response analyzer was used to study electrical conduction within the fluids since dielectric loss occurring at low frequencies under AC condition is dominated by mobile charge carriers. This is particularly important since power dissipation at power frequency, 50 Hz, may lead to dielectric heating. The dielectric response analyses of the samples within the range 10^{-3} - 10^{4} Hz showed a constant real relative permittivity at high frequency region. When the frequency dropped below 10^{1} Hz, interfacial polarization was observed at the electrode-liquid interface and this resulted in a significant dielectric increment in the real part of the relative permittivity at low frequencies with a negative slope greater than 1 and a frequency independent conductance (ε' slope = -1). This is an indication of Maxwell-Wagner interfacial effect where electric double layer (EDL) is formed. The real part acquired a slope of about -1 around frequency of 10^{-3} Hz. This suggests that the establishment of the EDL may be tending towards steady state. This change in the low frequency dispersion could be due to the ionic species undergoing interfacial electrochemical processes, or ions of lower mobility may have contributed to the EDL formation within the frequency region. This may have limited the effect of the strongly divergent processes at the interface.

Keywords: *charge transport, dielectric loss, electric double layer, dielectric liquid, frequency dispersion.*

1. Introduction

An understanding of the dielectric behaviour of insulating liquid requires the study of the dielectric response over a spectrum of frequency covering several decades and temperatures. Interfacial polarization is known to dominate measurements at low frequencies (frequency below 10^{-1} Hz); as a result, such measurement may reveal useful information about the charged particles in the liquid and their behaviour (Bartnikas, 1987). Dielectric loss is dominated by mobile charged carriers at low frequencies under AC conduction, the study of charge transport within an insulating fluid is particularly important since power dissipation at power frequency, 50 Hz, may lead to dielectric heating.

For a nearly perfect dielectric material, application of a sufficiently low alternating field produces no detectable phase difference (δ) between the voltage gradient ($\overline{E}$) and displacement vector $\left(\overline{D}\right)$. The ratio of the two vectors gives a constant value which is real and referred to as the relative permittivity. An ideal dielectric material has finite dielectric loss and in simple terms can be said to behave like parallel RC circuit (Figure 1). The values of R and C may be frequency dependent and the relative permittivity of the material becomes a complex quantity. The resistance R represents the lossy part of the dielectric which may result from electronic and/or ionic conductivity, dipole orientation, and space charge accumulation on the application of electric field. The storage capacity of the dielectric may be visualized the formation of dipole chains bound to counter-charges with their free ends on the surface of the plate s under the influence of applied electric field (Von Hippel, 1954).

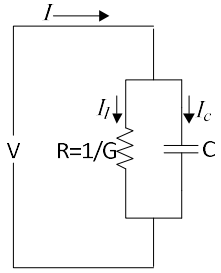

Figure 1: Parallel equivalent circuit of a dielectric

For a pure DC conduction in condensed matter, the real part of the relative permittivity, ε', is close to zero and independent of frequency. The acquisition of slope by ε' at low frequency in the log-log plot of real part, is due to polarizing species that is dominated by slow mobile charge carriers. While the slope of the imaginary part, ε'', with an approximate value of *-1* in a log-log plot of the imaginary part, ε" vs ω, is an indication of a low frequency dispersion (LFD). Low frequency dispersion can be volume or interfacial processes. While the presence of interfacial barrier layer at the electrode-sample interface is sometimes referred to as interfacial LFD, volume LFD is distributed throughout the thickness of the material. The loss in the material in this case is more than just a mere DC conduction. This type of response seems to be the lowest-frequency process observed in frequency response of dielectric material and has been termed the anomalous low-frequency dispersion (LFD) (Dissado *et al.*, 1984). The strong rise of ε' at low frequencies has a physical significance which

indicates a finite and reversible storage of charge in the bulk material or at the material-electrode interface (Raju, 2003). The curves of ε' and ε'' cross over at ω_c, the threshold frequency as shown in Figure 2. At a frequency below the threshold frequency, ω_c, ($\omega < \omega_c$), this response follows a fractional power law which is expressed as:

$$\varepsilon^*(\omega) = A(i\omega)^{n_2-1} = A[\sin(n_2\pi/2) - i\cos(n_2\pi/2)]\omega^{n_2-1} \quad 1$$

In this low frequency region $\varepsilon'' > \varepsilon'$, the frequency response is due to highly lossy "drift like" processes. The high frequency response, ($\omega > \omega_c$) may follow a similar power law but with the exponent equal to n_1 as expressed below. This is due to a low-loss "polarization like" process.

$$\varepsilon^*(\omega) = A(i\omega)^{n_1-1} = A[\sin(n_1\pi/2) - i\cos(n_1\pi/2)]\omega^{n_1-1} \quad 2$$

Where constant A is an empirical constant and n_1 and n_2 have value between *0* and *1* (Jonscher, 1996).

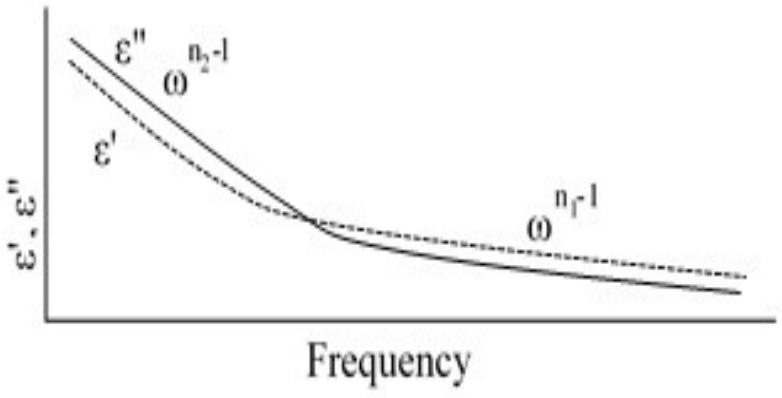

Figure 2: Low Frequency Dispersion (LFD) process (Raju, 2003)

This paper concentrates on the study of electrical conduction and loss characteristics of the ester derivatives using dielectric spectroscopy with a focus on low temperature and low frequency response. This is mainly to establish the dielectric behaviour of the material under electric field and the influence of processing steps on the ester derivatives at varied frequencies. It is known that during oil synthesis, remnant of some chemicals used for the ester synthesis are usually present in the ester sample. The remnants may undergo electrochemical processes and could constitute impurities in the samples. It has been established that Dielectric Spectroscopy is highly sensitive to small changes in electrical properties arising from presence of impurities in dielectric fluids. As such, it could provide a means of identifying the influence of synthesis steps in the dielectric properties of the ester derivatives. It could be possible to use the technique as analytical tool for investigating the influence of impurities on power dissipation responsible for overheating and premature failure of ester fluid.

2. Materials and Methods

2.1. Sample Preparation

An alkyl ester (PKOAE1) was synthesized from laboratory purified palm kernel oil by transesterification. Epoxy alkyl ester (PKOAE2) was then synthesized by epoxidation of PKOAE1 with an insitu peracetic acid (Abdelmalik *et al.*, 2011). Branched alkyl esters (PKOAE3 and PKOAE4) were then prepared using an acid-catalyzed ring-opening reaction of PKOAE2 with acid anhydrides in the presence of nitrogen (Sharma, *et al.*, 2008). Sample descriptions are summarized in Table 1. The samples were dried by degassing at reduced pressure in a vacuum oven at temperature of 85˚C for 2 hours.

Table1: Sample Description

Sample	Description
PKOAE1	Palm kernel oil methyl ester
PKOAE2	Palm kernel oil epoxy methyl ester
PKOAE3	Palm kernel oil methyl ester with C-3 carbon side branched chain
PKOAE4	Palm kernel oil methyl ester with C-4 carbon side branched chain
BS148	Mineral Insulating Oil

2.2. Structural Identification

Natural ester consists of fatty acids of various chain lengths. The synthesis involves a change in the chemical structure through modification of some of the fatty acids' chains in the ester. It is necessary to monitor the chemical reaction to know if the required products are obtained and identify the functional groups in the synthesized esters. This was achieved using Fourier Transform Infrared (FT-IR) Spectroscopy with the help of Perkin Elmer Spectrum One FT-IR spectrometer. The spectrometer sample holder and the cap were cleaned with methanol and acetone thoroughly. The cap was fixed and a background scan was carried out. A drop of the sample was placed on the spectrometer measurement cell. The sample was scanned with infrared radiation through frequency of 4000 - 650 cm^{-1} to obtain the spectrum. The amount of radiation absorbed by the sample was plotted as a function of the wave number of the absorbed radiation by a detector. Each spike (absorption bands) in the IR spectrum represents absorption of energy. The functional groups of the samples were identified from the spectra.

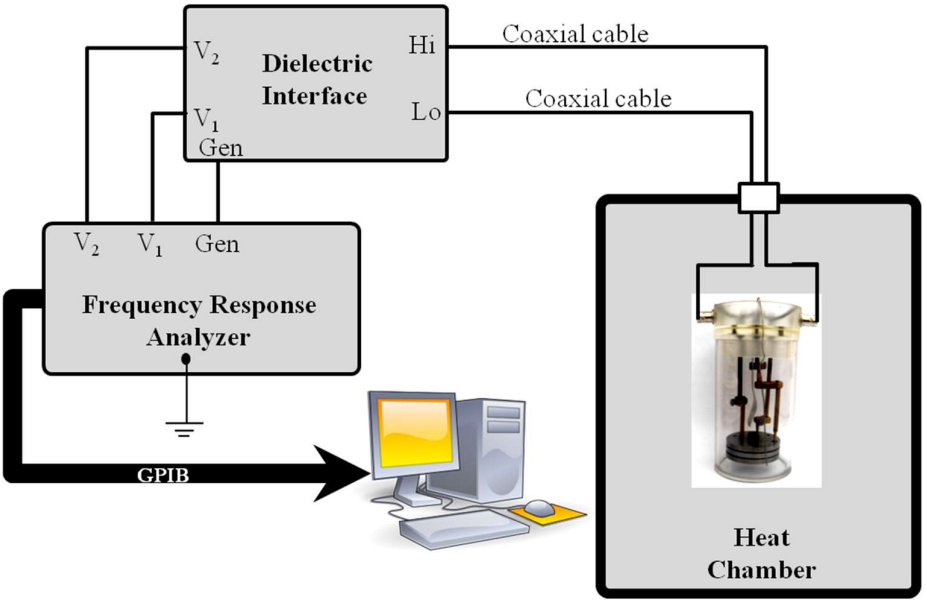

Figure 3: FRA experimental system for Dielectric Liquid

2.3. Dielectric Response Measurements

The dielectric properties of the samples were measured in a bespoke test cell designed such that the electrodes were suspended in the oil sample and had enough space to accommodate sample expansion (Abdelmalik *et al.*, 2012). The dielectric response of the samples was measured using a Solartron 1255 Frequency Response Analyzer and 1296 Dielectric Interface as shown in Figure 2. Dielectric measurements were taken over the frequency range 10^{-3} Hz to 10^{6} Hz and at number of fixed temperatures within the range 20˚C to 80˚C. The temperature of the sample was varied to within 0.1˚C by placing the cell in a temperature-controlled oven.

3. Results and Discussion

3.1. Structural study

The FTIR spectra (Figures 4 and 5) displayed peaks that are characteristic of functional groups common to the ester samples. PKOAE2 exhibits peaks around 844 cm^{-1} (Carey, 2000) due to the presence of epoxy group in the palm kernel oil alkyl ester. These peaks are characteristic of ester that has been epoxidized. These can be regarded as fingerprints of epoxy alkyl ester as the peaks fall within the fingerprint region. The existence of the peaks at 844 cm^{-1} on the PKOAE2 spectra shows that the transesterification reaction (needed to further modify epoxy alkyl ester) occurred without degradation of the epoxy rings.

The reaction of the ester with butyric anhydride (PKOAE3) yields a FTIR peak at 1080 cm^{-1} as shown in Figure 5, which is attributed to a grafted C-3 side branched hydrocarbon chain. The peak for the grafted C-4 side branched hydrocarbon chain (PKOAE4) was observed at 930 cm^{-1} when the ester was reacted with propionic anhydride. These peaks are uniquely the fingerprints of the respective alkyl esters revealing a marked variation in their appearance on the FTIR spectra. The peaks are unique to the respective esters and they differentiate the two alkyl esters.

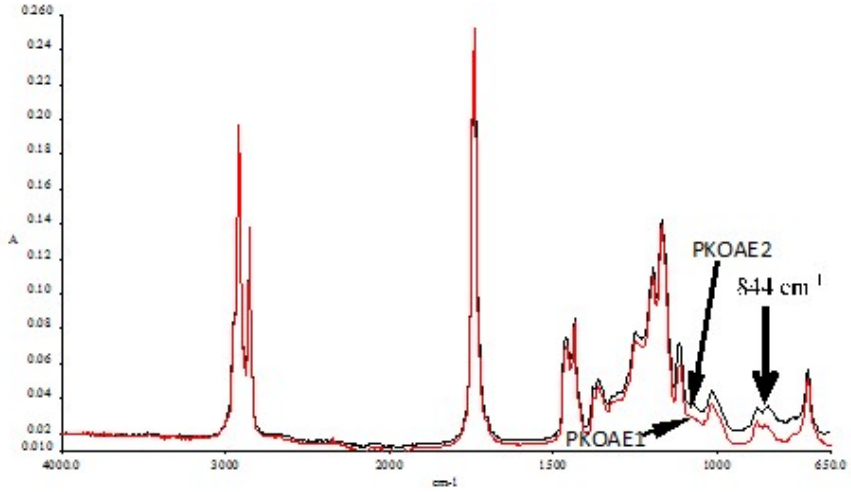

Figure 4: FTIR Spectra of PKOAE1 and PKOAE2

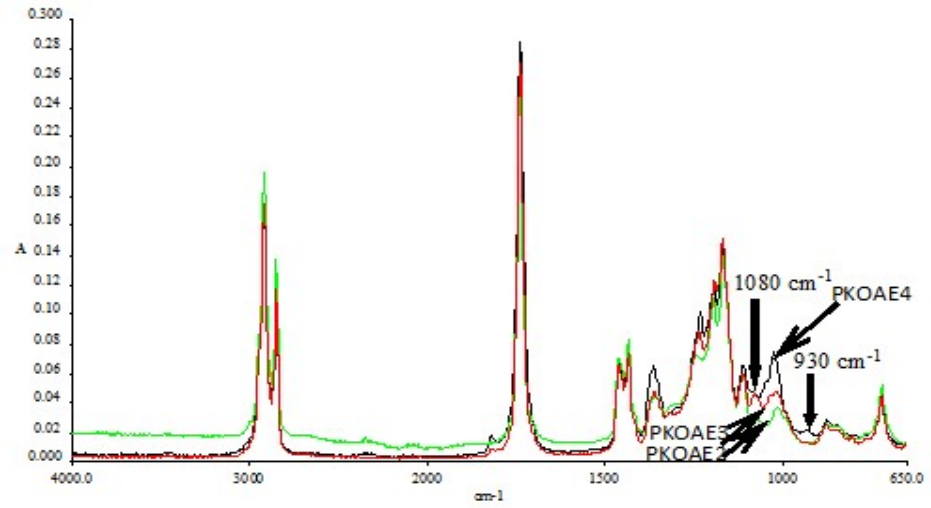

Figure 5: FTIR Spectra of PKOAE1, PKOAE3 and PKOAE4

3.2. Frequency Response Analysis

Previous study on the palm kernel oil-based ester fluid showed that it has properties ideally suited for use as alternative bio-based insulating fluid. The study also revealed the ester derivative to possess a flash point that matches the specified minimum flash point for mineral oil. Compared to mineral oil, the ester derivative of palm kernel oil is also paraded with higher thermo-oxidative stability, high and reliable breakdown strength (from the distribution of breakdown data of 43 kV/mm) with lower melting point of about -7˚C (Abdelmalik *et al.*, 2011), (Abdelmalik *et al*. 2012). The dielectric response of the synthesized esters measured above a frequency of about 10^{-2} Hz shows that the real part is constant (i.e. independent of frequency) and the imaginary part is inversely proportional to frequency. This is symptomatic of a constant capacitance in parallel with a constant conductance – that is, a constant electrical conduction mechanism dominates in this frequency range. At lower frequencies, the real part acquires a negative slope greater than 1 at 10^{-2} Hz whilst the imaginary part still maintains a slope of -1. This is indicative of interfacial polarization (Schmidt, 1994) with a more complex low frequency response. Temperature variations often influence the response of dielectric materials on the application of electric field. This change in temperature may lead to variation in the individual relaxation times. This usually results to a shift of the respective tan δ peak along the logarithmic frequency axis. The effect of temperature on the characteristic frequency of materials can be studied with a single curve known as master curve. This curve is constructed by normalizing the data for different temperatures. This is done by shifting the spectra for different temperatures into coincidence. If there are more than one process, e.g. a DC conduction and an (AC) polarization processes, and if these processes have different dependences on temperature, then it will only be possible to bring that part of the spectra corresponding to one process into coincidence with others having more than one processes employing a logarithmic shift procedure. In view of this, a logarithmic shift was performed on the frequency response of the alkyl ester samples to produce Master curves for these samples by using DC conduction to bring the spectra into coincidence The spectrum at 20˚C was chosen as the reference while the spectra at other temperatures were shifted towards it. The magnitude of the shift was invariant and as a result, the logarithmic shift along the frequency axis was carried out with the relation:

$$shift\ factor = \log a_T = \log(\omega_i) - \log(\omega_{ref}) = \frac{E_a}{k}\left(\frac{1}{T_{ref}} - \frac{1}{T_i}\right) \quad 3$$

Where $\log a_T$ is the logarithmic shift between any two frequencies, ω_{ref} and ω_i along the frequency axis corresponding to the same magnitude of the dielectric response function at T_{ref} and T_i. E_a is the activation energy.

Both real and imaginary parts are inter-dependent from Kramer Kronig relation; as a result, equation (3) was applied to both the real and imaginary part of the relative permittivity (Jonscher, 1983). The obtained master plots of the real and imaginary components of the relative permittivity as a function of frequency (i.e. a Bode plot) of the alkyl esters of palm kernel oil are shown in Figure 6 through Figure 9. The frequency response displayed a departure from simple Debye type relaxation. The real part is constant (i.e. independent of frequency) above approximately 10^{-1} Hz, while the imaginary part is inversely proportional to frequency with a slope of -1. This behaviour is an indication of a conduction mechanism dominating in this frequency range.

The low frequency wing of the real part was found not to match with each other, suggesting a different temperature dependent process. PKOAE1 has lower conductance compared with the other ester samples. The charges responsible for conduction in the liquid result from the dissociation of ionic and solid impurities in the liquid. Impurities introduced into the sample during processing may have contributed to the conduction current. At frequencies, below 10^{-1} Hz, the imaginary part maintains a slope of -1, and the real part of the relative permittivity acquires a slope between -1 and -2. This is still an indication of a strong dispersive behavior (interfacial polarization), an effect arising from the capacitive layer near the electrode.

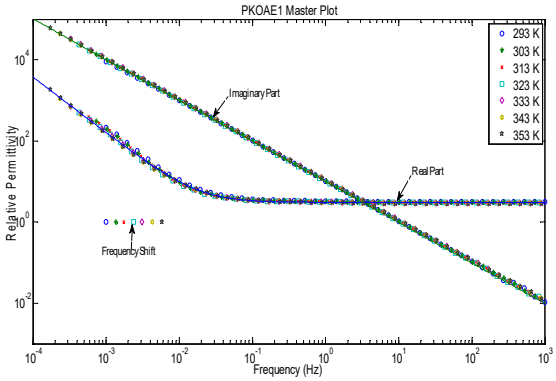

Figure 6: Master Curve for Dielectric Response of PKOAE1 (Solid line is a trend line)

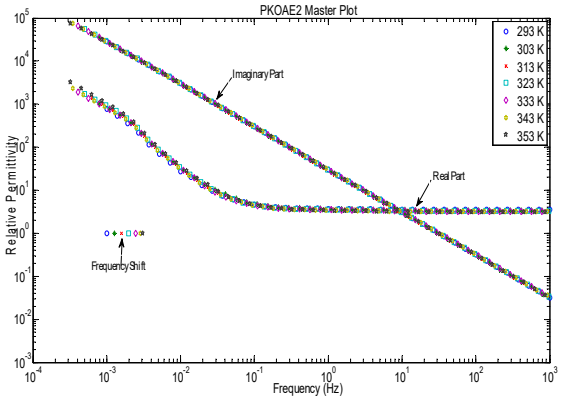

Figure 7: Master Curve for Dielectric Response of PKOAE2

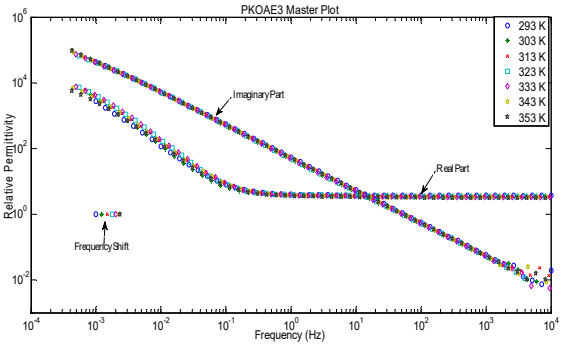

Figure 8: Master Curve for Dielectric Response of PKOAE3

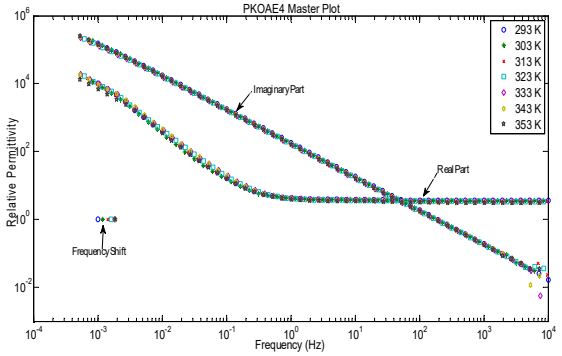

Figure 9: Master Curve for Dielectric Response of PKOAE4

The ionic species in the fluid drifted to the electrode-liquid interface and eventually accumulate near the electrode surface. The reversal of the applied electric field usually leads to the redistribution of these accumulated charges and this results to the establishment of a new equilibrium. Under constant electric field, a double layer is formed and is thought to be made up of several "layers". In a liquid such as alkyl esters with low conductivity, it is assumed that two layers exist at the electrode (Schmidt, 1994). The closest layer to the electrode is referred to as the Stern layer. This is a compact layer of ions next to the electrode. The double layer of the ester samples may have contained the oil molecules and ionic species. Following the Stern layer is a layer of ions that are distributed in a three dimensional region called the diffuse layer. This layer is also referred to as Gouy Chapman layer (See Figure 10). This layer extends into the bulk liquid because of the counter actions of electrostatic field and thermal agitation in the liquid. At higher frequencies, the time scale was too short for the ions to align to form the electric double layer (EDL) at the electrode liquid interface. As the frequency drops below 10^1 Hz, the ions have much longer time to align themselves forming the EDL. The formed double layer contributed a finite value that results in increase in the real part of the capacitance.

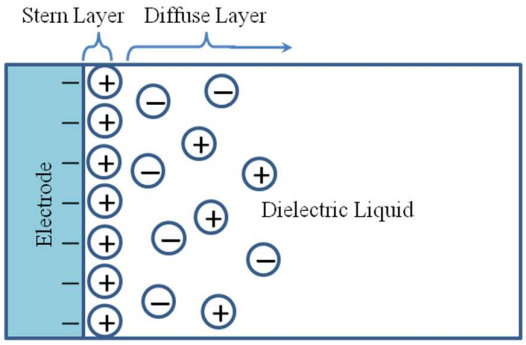

Figure 10: Model of Electric Double Layer

PKOAE2, PKOAE3 and PKOAE4 appeared to exhibit similar behaviour with PKOAE1. But a close inspection of the spectra revealed that, the real part of dielectric response of the esters undergoes a change below the frequency of 10^{-1} Hz. A very slow response was observed on the real part of the relative permittivity with an approximate slope of -1. The low frequency dispersion is equivalent to a dispersive barrier in series with the bulk conductance. However, the dispersive barrier appeared to have a more complex behaviour compared with the behaviour of PKOAE1 sample within the frequency range studied. At the onset of electrode polarization phenomenon, the frequency dependence of the real relative permittivity is proportional to ω^{n-1}, where the value of n is between 0.45 and 0.65 for the three samples. This slope gradually changes to about -1 at lower frequencies. This suggests that the establishment of the EDL may be tending towards steady state. This change in the low frequency dispersion could be due to the ionic species undergoing interfacial electrochemical processes (Raju, 2003), or ions of lower mobility may have contributed to the EDL formation within the frequency region. Variation in the thickness of the layer at the

electrode-liquid interface may also have caused the change in the slope of the real part of the dielectric response at lower frequencies.

3.3. Arrhenius Behaviour of Frequency Response

Information on the influence of thermal energy on the behaviour of the double layer can be extracted from the relaxation frequency. The influence of temperature on the characteristic frequency was determined with equation 3. The plot of the characteristic frequency shifts in the dielectric response of PKOAE1, PKOAE2, PKOAE3, and PKOAE4 is shown in Figure 11.

The real and imaginary parts of relative permittivity of ester samples obey simple Arrhenius behaviour with correlation coefficients (R^2) ranging from 0.96 to 0.99. The ester samples displayed systematic linear shift in the characteristic frequency with increasing temperature. As a result, the activation energies for samples PKOAE1, PKOAE2, PKOAE3 and PKOAE4 were determined from the slope of the Arrhenius plots of their characteristic frequency shifts to be 0.27 *eV*, 0.18 *eV*, 0.13 *eV*, and 0.08 *eV* respectively. The relaxation time of electrode polarization expressed as [4];

$$\tau_{EP} \propto \frac{1}{T}\exp\frac{c}{kT} \qquad 4$$

decreases with increasing temperature; where c is a constant for a given liquid. The systematic shift in the relaxation frequency towards higher frequency may be due to changes in the relaxation time of electrode polarization with increasing temperature.

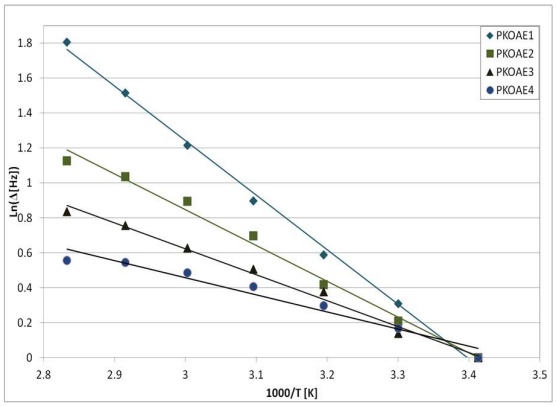

Figure 11: Characteristic Frequency Shift of Ester Dielectric Response on Arrhenius Axes

Electrical conductivity, σ_{ac} is related to the imaginary part of the relative permittivity, ε", with the expression:

$$\sigma_{ac} = \omega\varepsilon'' \qquad 5$$

where ω is the angular frequency. The AC conductivity of PKOAE1, PKOAE2, PKOAE3 and PKOAE4 calculated using equation 5 is plotted on Arrhenius axes in Figure 12. The electrical conductivity was evaluated from the imaginary part of the frequency response data of the samples within the temperature range of 20˚C to 80˚C. The straight lines obtained indicate thermally activated transport mechanisms. The activation energies of PKOAE1, PKOAE2, PKOAE3 and PKOAE4 derived from these Arrhenius plots are shown in Table 2. The dielectrics appears to be losing its insulating properties (i.e., emergence of pronounced ionic conduction which is referred to as dielectric loss) as a result of thermally activated process. The calculated conductivity increased from PKOAE1 through PKOAE4. The conductivity is relatively constant with frequency as was reported by Bartnikas for most insulating liquids (Bartnikas, 1994).

The dielectric response of the synthesized esters has LFD-type interfacial behaviour. The samples become more viscous as we progress from sample with unsaturated fatty acids to fatty acids with epoxy group to fatty acids with side branch chain. The conductivity also increases. Since mobility decreased with increasing viscosity, it follows from the conductivity expressed in equation 5 that an increase in the concentration of conducting impurities introduced during the processing could be responsible for the increase in the electrical conductivity. This increased concentration may have resulted from impurities formed or introduced during the processing stages. A filtering process that will be able to eliminate these conducting impurities will improve the insulating properties.

The dielectric dispersion of the oil increases with temperature due to decreased viscosity arising from temperature variation. Mobility enhancement of the charged particles was due to decreased (Bartnikas, 1994). This ease in the mobility of more charged carriers results in more mobile charged carriers contributing to the loss phenomena at higher temperatures. This effect is responsible for the gradual increase in the conductivity of the oil as viscosity decreases.

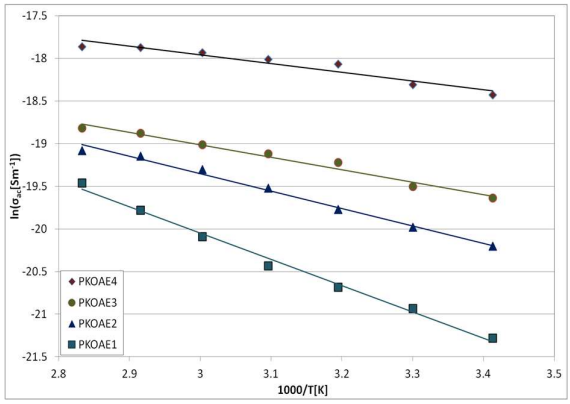

Figure 12: Plot of Electrical Conductivity of Ester samples on Arrhenius Axes

Table 2: AC Conductivity and Activation Energy

Samples	σ_{AC} *(S/m)*	*Activation Energy for* σ_{AC} *(eV)*
PKOAE1	5.72×10^{-10}	0.27
PKOAE2	1.68×10^{-9}	0.18
PKOAE3	2.95×10^{-9}	0.13
PKOAE4	9.89×10^{-9}	0.10

The dispersive barrier formed in the ester samples appeared to have a complex behaviour. The plot of the response of the ester samples in complex impedance plot is shown in Figure 13. It clearly displayed a separation of the bulk mechanism from the interfacial phenomenon. The semicircular-like arc occurring at high frequency region indicates that conductance is the dominant

process in the bulk material, while the spurs resulted from the interfacial phenomenon which includes interfacial polarization and a suspected electrochemical or low ionic mobility processes. This means that charge-transfer kinetics alone dictates the conduction process at high frequency region.

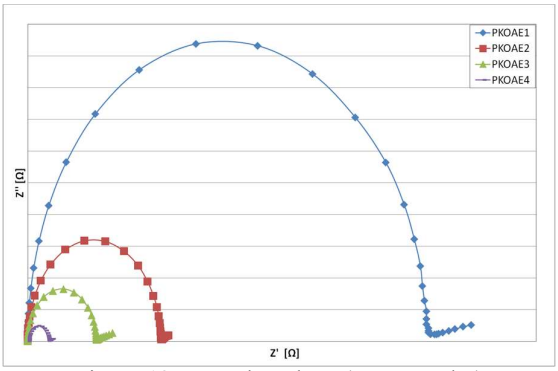

Figure 13: Complex plane (Z" vs Z' plot)

The area under the semicircular arc reduces as the conductivity of the samples increases. To understand the physical interpretation of the arc, let us consider a parallel R-C circuit to represent the bulk liquid and the double layer to involve two parallel processes that consists of the double layer capacitance, C_n and polarization resistance, R_n. At a very high frequency, the contribution from the double layer to the imaginary part of the impedance is zero. As the frequency decreases, the contribution from C_n becomes finite. C_n then gives a high reactance and the current passes predominantly through the bulk conductance and polarization resistance. This overall effect is an increasing Z' and diminishing Z''. There exists a transition between the semicircular arc and the inclined spur for the respective ester samples. The lowest value for the imaginary part of the impedance corresponds to frequency of $tan\ \delta$ peak. This is the relaxation frequency for electrode polarization ionic species and the corresponding relaxation time can be evaluated from it. The frequency dependence of this region is only from interfacial polarization. At lower frequencies when $\omega \rightarrow 0$, the electric double layer becomes dominant and low frequency dispersion as indicated by a low frequency power law, played a significant role in the dielectric response of the material. Interfacial dispersion may be responsible for the nature of the response obtained for the alkyl esters. This response can be represented as a dispersive barrier in series with parallel bulk R-C as shown in Figure 14. The frequency dependent dispersive barrier is dipicted as a component in series with a parallel combination of polarization resistance, R_n ($1/G_n$) and capacitance, C_n in Figure 14 (Bret et al., 1993; Bard et al.,2001).

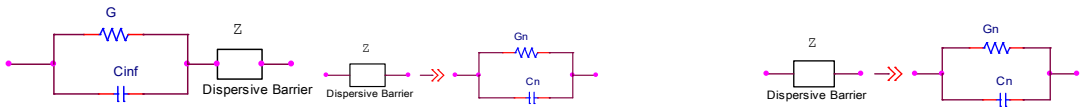

Figure. 14: Equivalent Circuit for Electrode Polarization in Alkyl Ester

4. Conclusions

The dielectric characterization of the synthesized samples was performed over the frequency range 10^{-3} - 10^{6} Hz and at a number of fixed temperatures. The temperature ranges from 20˚C to 80˚C at an interval of 10˚C. The measurements results presented on master plots enabled the observation of the dielectric responses of the samples down to a frequency of 10^{-4} Hz at 20ºC. Ion transport in the ester samples is a thermally activated process with obtained activation energies that varied between 0.08 *eV* and 0.27 *eV*. The activation energy decreased as the oil sample was modified from fatty acids containing unsaturated nature to the conversion of the C-C double bond to epoxy ring and to grafting of side branch chain. The esters displayed strong low frequency dispersion (LFD). The impurity charge carriers in the fluids influenced the real part of the relative permittivity, ε' at very low frequencies (< 10^{-1} Hz). Although the synthesized esters possessed low viscosity, they have higher conductivity compared with the existing insulating fluids. These properties may have resulted from an increase in concentration of impurity charges and/or high mobility due to low viscosity.

5. Acknowledgements

I wish to acknowledge Islamic Development Bank for sponsoring this work. The support of National Grid UK is also acknowledged. The contributions of Prof. J.C. Fothergill, London City University, UK and Dr. S.D. Dodd, University of Leicester, UK is acknowledged.

6. References

Abdelmalik A.A., Abbott A.P., Fothergill J.C., Dodd S., Harris R.C. (2011). Synthesis of a base-stock for electrical insulating fluid based on palm kernel oil. Industrial Crops and Products, 33, 532–536.

Abdelmalik A.A., Fothergill J.C., Dodd S.J. (2012). Electrical conduction and dielectric breakdown characteristics of alkyl ester dielectric fluids obtained from palm kernel oil, IEEE Transactions on Dielectrics and Electrical Insulation, 19(5), 1623-1632.

Bard A.J., Faulkner L.R. (2001). Electrochemical methods: fundamentals and applications. 2ed, John Wiley & Sons, Inc.

Bartnikas, R. (1987). Alternating-current loss and permittivity measurements, In: Bartnikas R. Engineering Dielectric, Vol. IIB, Electrical properties of solid materials: Measurement techniques, ASTM Publication 1987; 52-123.

Bartnikas R. (1994), Permittivity and loss of insulating liquid. In: Bartinikas R. Engineering dielectrics, Vol. III, Electrical insulating liquids, ASTM Publication, 3-146.

Brett C.M.A., Brett A.M.O. (1993). Electrochemistry: principles, methods, and applications. Oxford University Press.

Carey F.A. (2000). Organic chemistry, 4ed., McGraw Hill Higher Education, Boston.

Dissado, L.A. Hill R.M. (1984). Anomalous low-frequency dispersion, J. Chem. Soc., Faraday Trans, 2(80), 291-319.

Jonscher A.K. (1983). Dielectric relaxation in solids, Chelsea Dielectric Press, London.

Jonscher A.K. (1996), Universal Relaxation Law, Chelsea Dielectric Press Ltd, London.

Raju G.G. (2003). Dielectrics in Electric Fields. Marcel Dekker, Inc.

Schmidt W.F. (1994). Conduction mechanism. In: Bartnikas R., Liquids in engineering dielectric, Vol. III, Electrical Insulating Liquids. ASTM Publication, 147-260.

Sharma B.K, Liu Z., Adhvaryu A. and Erhan S.Z. (2008). One-Pot Synthesis of chemically modified vegetable oils, *J. Ag. Food Chem.,* 56, 3049-3056.

Von Hippel, A.R. (1954). Theory. In: Von Hippel A. R. Dielectric Materials and Applications, Massachusetts, The MIT Press, 3-46.